

Static impurities in the $S=1/2$ kagome lattice: Dimer freezing and mutual repulsion

S. Dommange,¹ M. Mambrini,² B. Normand,³ and F. Mila⁴

¹*Institut Romand de Recherche Numérique en Physique des Matériaux (IRRMA), PPH–Ecublens, CH-1015 Lausanne, Switzerland*

²*Laboratoire de Physique Théorique, Université Paul Sabatier, FRE 2603, F-31062 Toulouse Cedex, France*

³*Département de Physique, Université de Fribourg, CH-1700 Fribourg, Switzerland*

⁴*Institute of Theoretical Physics, Ecole Polytechnique, Fédérale de Lausanne, CH-1015 Lausanne, Switzerland*

(Received 11 June 2003; published 17 December 2003)

We consider the effects of doping the $S=1/2$ kagome lattice with static impurities. We demonstrate that impurities lower the number of low-lying singlet states, induce dimer-dimer correlations of considerable spatial extent, and do not generate free spin degrees of freedom. Most importantly, they experience a highly unconventional mutual repulsion as a direct consequence of the strong spin frustration. These properties are illustrated by exact diagonalization, and are reproduced to semiquantitative accuracy within a dimer resonating-valence-bond description which affords access to longer length scales. We calculate the local magnetization induced by doped impurities, and consider its implications for nuclear magnetic resonance measurements on known kagome systems.

DOI: 10.1103/PhysRevB.68.224416

PACS number(s): 75.10.Jm, 75.30.Hx, 76.60.–k

I. INTRODUCTION

The kagome geometry (Fig. 1) presents one of the most highly frustrated quantum spin systems achievable in two dimensions (2D) with only nearest-neighbor Heisenberg interactions. The $S=1/2$ kagome lattice has been found to have a spin-liquid ground state,¹ whose ultrashort spin-spin correlation lengths are effectively those of a dimer liquid,^{2,3} and whose excitation spectrum⁴ shows a manifold containing an extremely large number of low-lying singlets.⁵ These properties are reproduced very well by a short-range resonating-valence-bond (RVB) description,⁶ based in fact only on nearest-neighbor dimer formation (Fig. 1).

On the theoretical level, a similar degree of frustration is found only in quantum dimer models,^{7,8} which have also been considered recently in the kagome geometry,⁹ and in models containing higher-order spin terms and multiple-spin exchange.¹⁰ Experimentally, a variety of materials displaying the kagome structure is known to exist, although to date none have been found which contain an ideal, 2D, vacancy-free system of spins $S=1/2$. These include the jarosites $(\text{H}_3\text{O})\text{Fe}_3(\text{OH})_6(\text{SO}_4)_2$,¹¹ $\text{KFe}_3(\text{OH})_6(\text{SO}_4)_2$, and $\text{KCr}_3(\text{OH})_6(\text{SO}_4)_2$ (Refs. 12 and 13), and the volborthite $\text{Cu}_3\text{V}_2\text{O}_7(\text{OH})_2 \cdot 2\text{H}_2\text{O}$.¹⁴ The best characterized of these compounds is the magnetoplumbite $\text{SrCr}_9\text{Ga}_{12-9p}\text{O}_{19}$ (SCGO),¹⁵ in which some of the $S=3/2$ Cr^{3+} ions form approximately 2D kagome planes. However, because in this case the ideal stoichiometry ($p=1$) remains unachievable, discussion of the influence of static (and also, for Ga^{3+} , spinless) impurities represents an important issue.

Studies of static vacancies in spin liquids have tended to focus on the question of induced free spin degrees of freedom.¹⁶ In systems such as spin ladders, and also for the 2D square lattice,¹⁷ the total energy appears to decrease as such holes in the spin background are made to approach each other, implying an effective mutual attraction. It is generally believed that in a RVB description of the ground state the minimal disruption of the wave function, and thus the most favorable energy state, occurs when holes occupy adjacent

sites, thus generating a simple pairing mechanism for mobile dopants. The issue of impurities in frustrated magnets has received less attention, and appears to be more involved: it has been proposed that an absence of induced free spins corresponds to deconfined, spinonlike excitations.¹⁸ Consideration of the problem for the 1D frustrated chain,¹⁹ which provides an example with no free spins localized around the vacancies, suggests the importance of degenerate singlets in the ground-state manifold. This result indicates that the kagome geometry presents the most probable candidate for exotic behavior²⁰ as a consequence of strong frustration in 2D. A numerical analysis, similar to the type performed here but restricted to the singlet-triplet gap, has been used to argue that such behavior does indeed include deconfined spinon excitations.²¹

In this study we investigate the effects of static impurities in the kagome lattice. We find that, despite the very short intrinsic spin-spin correlation lengths, dimer-dimer correlations develop over considerable distances in the presence of

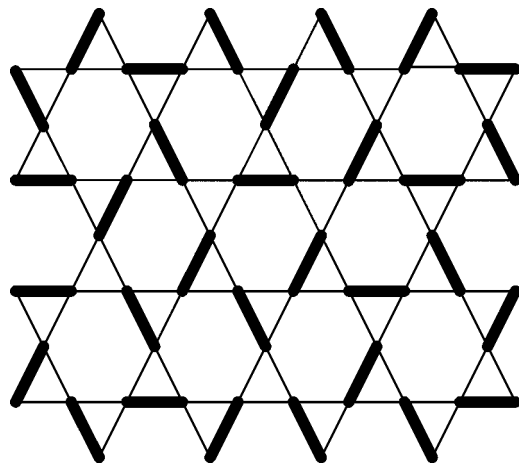


FIG. 1. The kagome lattice. Thick black lines represent an arbitrarily chosen covering by nearest-neighbor dimers formed between $S=1/2$ spins on each lattice site.

dopants. Further, we show that there is no evidence for free local moments induced around impurity sites, and that a highly unusual effective repulsive interaction arises between such holes in the spin background.

In Sec. II we provide an outline of the numerical and analytical methods to be employed, and discuss the fundamental effects on the excitation spectrum of doping by spinless impurities. In Sec. III we consider the case of one hole in an odd-site cluster, demonstrating “dimer freezing” in the spin-spin correlation functions and dimer-dimer correlations of anomalously long range. The induced magnetizations in the spin sectors $S=1$ and higher are used to illustrate the consequences for nuclear magnetic resonance (NMR) measurements. Section IV presents spin-spin correlation functions which characterize the situation with two impurities, supplemented by total-energy analyses quantifying the novel repulsive interaction between the holes which emerges from this study. Section V contains further discussion and our conclusions.

II. ELIMINATION OF SINGLET STATES AND ABSENCE OF LOCALIZED SPINS

A. Exact diagonalization

By “impurity” we refer henceforth to nonmagnetic impurities. The techniques we employ are based primarily on numerical calculations for small clusters with periodic boundary conditions chosen as symmetrically as possible. Specifically, we perform exact diagonalization (ED) studies of the Heisenberg Hamiltonian

$$H = J \sum_{\langle ij \rangle} \mathbf{S}_i \cdot \mathbf{S}_j, \quad (1)$$

where J is the antiferromagnetic superexchange interaction and $\langle ij \rangle$ denotes nearest-neighbor sites, for clusters up to 27 sites with one impurity and up to 24 sites with two impurities for all available configurations. We analyze the total energies, the energies per doped impurity, and also the form of the energy spectra, focusing on the number of singlet states in the low-energy manifold below the first triplet for the finite systems under consideration, as well as on the number of these states removed by impurity doping. The frustrated spin interactions in the presence of impurities are characterized for the entire cluster by the bond spin-spin correlation functions and by the induced site magnetizations in every spin sector.

The density of states integrated over the lowest-lying energy levels is shown in Fig. 2 for systems with and without impurities. Figure 2 compares ED results from systems of 18 sites, for which in the impurity configuration illustrated 8 of the 12 singlet states occurring below the first triplet, indicated by the vertical lines, are eliminated by the presence of two impurities. Although the separation of the triplet from the lowest remaining singlet decreases, this energy gap remains a finite fraction of the superexchange interaction J for any impurity configuration, as shown also in Ref. 21. Thus the most important qualitative result emerging even for the

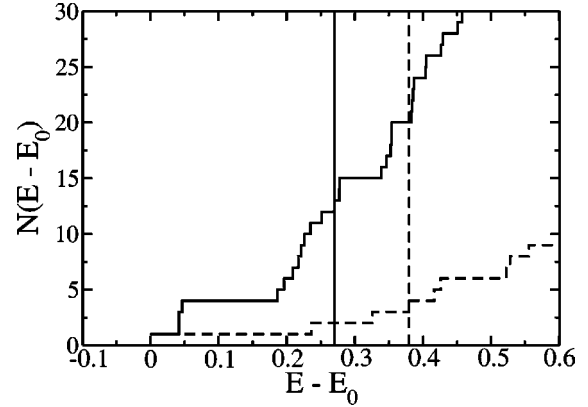


FIG. 2. Integrated density of states for an 18-site $S=1/2$ kagome cluster, computed by exact diagonalization both without impurities (solid line) and with two impurities (dashed line). The vertical lines mark the position of the first triplet state in the absence of impurities (solid) and in their presence (dashed).

smallest systems is that, in contrast to unfrustrated spin-ladder and dimerized or quadrumerized systems, no low-lying triplet state is induced by the presence of impurities. This implies directly¹⁹ that there are no quasifree spin degrees of freedom, by which is meant spins effectively isolated from their local environment and interacting with each other only on an effective energy scale much smaller than J .

The fact that no localized moments are formed in the vicinity of impurities may be ascribed to the continuum of singlets extending above the ground state, which has the same function as the twofold degeneracy of the ground state in the frustrated chain,¹⁹ namely that the rearrangement of dimers incurs no energy penalty. In this context we note the fact that the picture of a continuous manifold of low-energy singlets has been challenged, in particular by recent suggestions²² that valence-bond-ordered ground states may arise with unit cells of 12 or 36 sites. At present the reliability of such predictions remains unclear, and, as discussed in Sec. IV below, our two-hole results do not favor such a possibility. The presence of a very small gap in the singlet manifold would in any case affect the physics only for very large impurity separation by causing a weak confinement of $S=1/2$ spins in the vicinity of the vacancies, a result which it is not possible to investigate by numerical techniques given currently available system sizes for ED. However, the upper bound for the hypothetical gap in the singlet manifold set by the analyses of Ref. 4 indicates that for impurity concentrations in excess of a fraction of a percent, the development in the clean system of valence-bond order is not relevant, and the present considerations are expected to be valid. This statement is supported by our results for small to intermediate impurity separation, which show that spin-1/2 degrees of freedom “liberated” by the creation of vacancies indeed recombine into singlets. This absence of local spins around nonmagnetic impurities represents one of the most significant differences between frustrated and unfrustrated systems, and has been further interpreted as implying a deconfinement of the spin degrees of freedom.¹⁸

Table I provides more details of the number of states in

TABLE I. Number of low-lying singlets below the first triplet for kagome clusters without impurities (N_s^0 , third row) and with two impurities (N_s^2 , fourth row) as a function of the Manhattan distance d_M between impurities. Results obtained by ED are shown for clusters of $N = 12$ and 18 sites.

N	12				18				
d_M	1	2	2	3	1	2	2	3	3
N_s^0	4	4	4	4	12	12	12	12	12
N_s^2	2	2	3	1	3	4	4	3	4

the singlet manifold which are removed by impurity doping for clusters of 12 and 18 sites, for all possible configurations of two impurities. The numbers vary little as a function of the proximity of the impurities, and the average number of low-lying states which are eliminated is in agreement with simple considerations of the number of singlet states in the small system (below). We have also performed analogous calculations for 24-site clusters of different shapes. For all clusters the same behavior is found upon introducing two impurities, in that the number of singlets below the first triplet is reduced, but here the lowest-lying excitation is not a triplet. However, these clusters do not appear to be representative of the generic kagome physics, as the number of low-lying singlets in the absence of impurities is significantly smaller than the expected value⁴ of 1.15^N . This situation is presumed to be a consequence of the low symmetry of the 24-site clusters, some of which are essentially 1D systems, and as a result the densities of states are not presented here.

B. Dimer-RVB basis

We calculate in addition the ground-state properties, namely the energy and spin-spin correlation functions, of clusters doped with one and with two impurities within the dimer-RVB basis. This is the basis of states in which every spin forms a singlet dimer with one of its nearest neighbors in such a way that every spin of the lattice is involved in a dimer (Fig. 1). The use of this basis⁶ naturally implies a truncation of the total number of available states in the manifold of low-lying singlets, but we will show below that it provides a satisfactory description of the ground state of the doped system. Dimer-RVB calculations permit the consideration of somewhat larger cluster sizes, and we will present results up to and including 39 sites with one impurity and 36 sites with two impurities.

Calculations performed in the dimer-RVB basis yield results very similar to the exact ones for the integrated density of states (Fig. 3), giving clear evidence of a strong linear correlation (see also Fig. 9) between the ED and dimer-RVB spectra in both 0- and 2-impurity cases. Demonstration of a quantitative correspondence between the spectra would require shift and scaling factors arising from an energetic renormalization related to the fact that calculations in the dimer-RVB basis are variational in nature, so that the true eigenstates are dressed RVB wave functions, but this procedure is not necessary for the analysis to be presented here.

Given that the RVB basis represents a very significant truncation of the total Hilbert space, the qualitative similarity

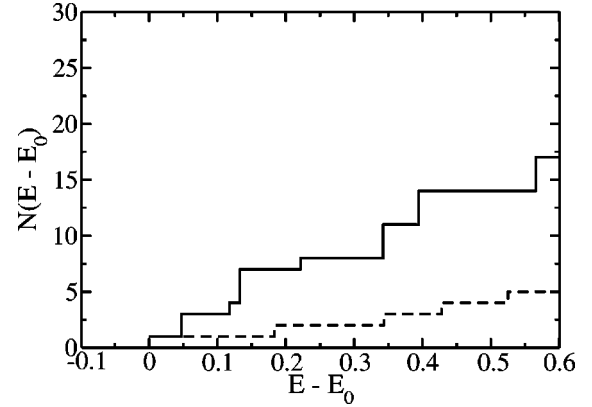


FIG. 3. Integrated density of singlet states for an 18-site $S = 1/2$ kagome cluster, calculated in the dimer-RVB basis both without impurities (solid line) and with two impurities (dashed).

of the dimer-RVB spectra to those obtained from the exact calculations, both with and without impurities, provides important information about the nature of the exact wave functions of the kagome system. This observation is further confirmed by the semiquantitative agreement with exact results for spin-correlation functions and ground-state energies computed using the dimer-RVB basis. We defer this comparison to Secs. III and IV, and comment here only that our results in the presence of impurities provide additional strong justification for the statement that the ground state of the kagome spin system is described appropriately by a maximally short-ranged RVB wave function, presumably as a consequence of the very strong frustration.

The dimer-RVB basis is a natural framework for understanding the absence of localized spins around an impurity site, as all remaining spins are simply incorporated within rearranged singlet dimer coverings. It also provides a qualitative reflection of the “evaporation” of low-lying singlets from the ground-state manifold (Figs. 2 and 3 and Table I) which arises on doping a cluster with two impurities, and in fact yields additional insight into the mechanism for this exclusion. It can be shown that the total number of singlet dimer coverings of a doped system is given by

$$N_{\text{coverings}} = 2^{N/3 - N_{\text{imp}} + N_G + N_{\text{et}}}, \quad (2)$$

where N is the number of sites of the system under consideration, N_{imp} the number of doped impurities, N_G the number of independent clusters into which the system is divided by the dopant distribution, and N_{et} the number of triangles containing three impurities. A complete derivation of this result lies beyond the scope of the current analysis, and we present only the following heuristic explanation. By reducing each triangle to an effective $S = 1/2$ degree of freedom,^{5,6} the dimer basis involves a truncation of the 2^N total states to $2^{N/3}$, multiplied by an additional factor of 2 for the overall spin direction on each independent cluster. Each added impurity removes one spin, halving the number of states in every manifold and thus justifying the dependence on N_{imp} . The only exception to this statement occurs when the added impurity falls on a triangle which already contains two im-

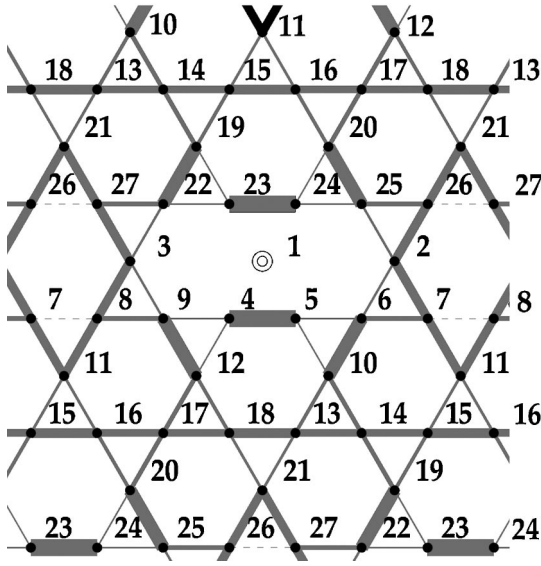


FIG. 4. Bond spin-spin correlations for a single impurity in a 27-site cluster, obtained by ED. Bar width represents the strength of correlation functions on each bond on a linear scale where the strongest correlation function is $\langle \mathbf{S}_i \cdot \mathbf{S}_j \rangle = -0.69$. Dashed lines denote bonds on which $\langle \mathbf{S}_i \cdot \mathbf{S}_j \rangle > 0$.

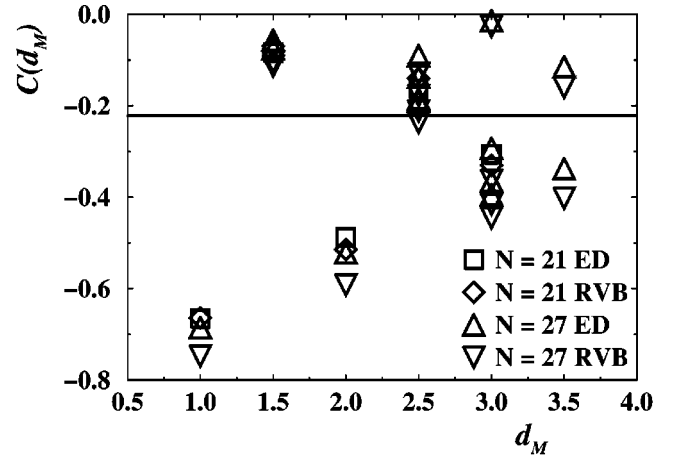
purities, as a result of which it is already fully constrained and removal of the third site no longer affects the number of coverings. Equation (2) can be shown to remain valid for all vacancy concentrations, including most notably values of N_{imp} exceeding the percolation threshold, beyond which N_G must exceed 1, under the condition that the impurity distribution does not cut the system into segments containing odd numbers of spins.

III. SPIN-CORRELATION FUNCTIONS AND INDUCED MAGNETIZATION

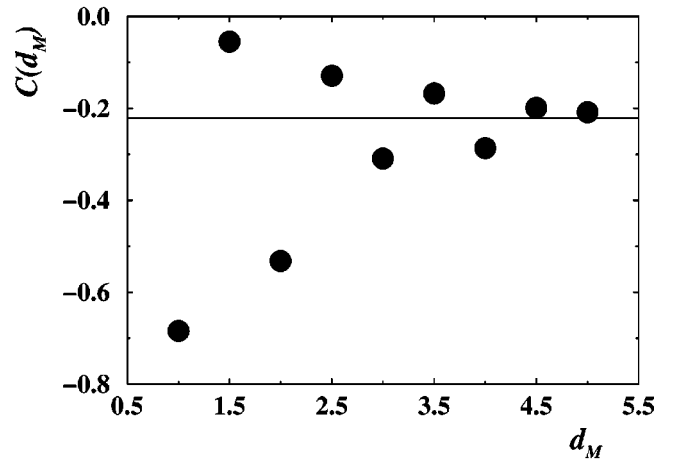
A. Dimer “freezing”

In this section we consider the effects of a single impurity introduced in an odd-site cluster. The bond spin-spin correlation functions $\langle \mathbf{S}_i \cdot \mathbf{S}_j \rangle$ around a single impurity may be computed by ED for clusters of up to 27 sites. The ED calculations permit in addition the determination of the magnetizations induced on each site by the presence of the impurity, with results for every spin sector corresponding to the situation in all applied magnetic fields, which are presented in a later subsection.

The correlation functions obtained by ED are illustrated in Fig. 4 for a 27-site cluster with periodic boundary conditions. The most striking feature of these results is that dimer bonds are effectively frozen in the two depleted triangles, taking a value $\langle \mathbf{S}_i \cdot \mathbf{S}_j \rangle \approx -0.69$ close to the theoretical minimum of $-3/4$ for a pure singlet state. For comparison, the average value of $\langle \mathbf{S}_i \cdot \mathbf{S}_j \rangle$ in the pure system, which retains full freedom to resonate, is a factor of 3 smaller (-0.22).² The bonds neighboring the frozen dimers then show very weak correlations, while the next neighbors are again enhanced, and the spin correlations oscillate with distance away from



(a)



(b)

FIG. 5. (a) Bond spin-spin correlation functions $C(d_M) = \langle \mathbf{S}_i \cdot \mathbf{S}_j \rangle$ on nearest-neighbor bonds as a function of their Manhattan distance d_M from a single impurity, for clusters of 21 and 27 sites. The site-bond separation d_M is obtained from the average of the Manhattan distances between the impurity site and the two sites constituting the bond. (b) Spin-spin correlations as a function of (Manhattan) bond distance from a single impurity, obtained by dimer-RVB calculations for a 39-site cluster. Points represent the average over all bonds at the same distance from the impurity, the solid line the value $\langle \mathbf{S}_i \cdot \mathbf{S}_j \rangle = -0.22$ for the impurity-free system.

the impurity [also illustrated in Fig. 5(b)]. Thus although bond spin-spin correlations in the kagome system are extremely short-ranged,² induced dimer-dimer correlations show a considerable spatial extent, reaching in fact well beyond the sizes obtainable by studying small clusters using either ED or dimer-RVB techniques. For the limited data available it is unfortunately not possible to specify the functional form of the decay to equilibrium. Further analysis of this issue, based on data obtained from mutual hole repulsion, is presented in Sec. IV.

B. Dimer-RVB basis

Figure 5(a) compares the bond spin-spin correlation values $\langle \mathbf{S}_i \cdot \mathbf{S}_j \rangle$ obtained from ED and from the dimer-RVB basis

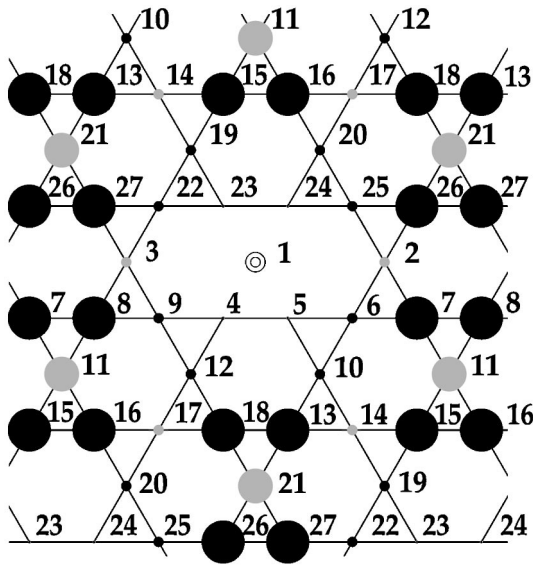


FIG. 6. Site magnetization profile of the lowest triplet state induced by a single impurity in a 27-site cluster, obtained by ED. Dot radius represents the magnitude of the local moment on a linear scale where the largest dot corresponds to a moment of $0.13 \mu_B$ ($0.5 \mu_B$ is the moment of a free electron), and the gray dots represent sites with induced moments opposite to the field.

for all bonds in clusters of 21 and 27 sites with one impurity. These clusters represent the maximal sizes accessible by ED, and for such systems it is clear that the dimer-RVB basis reproduces the exact values with quantitative accuracy. From the nature of the RVB basis it is perhaps to be expected that nearest-neighbor bond correlations are treated more accurately than any other physical property. We make use of this feature to extend the calculations of spin-correlation functions to a system of 39 sites with one impurity. Because on this cluster the boundary conditions lead to a rather low symmetry, Fig. 5(b) shows the value of $\langle \mathbf{S}_i \cdot \mathbf{S}_j \rangle$ averaged over all bonds at the same Manhattan distance from the impurity, which illustrates both the oscillatory nature of the frozen dimerization pattern and the very long range over which an impurity acts to disrupt the spin configuration.

C. Induced magnetic moments

The local magnetization pattern induced in the vicinity of a doped nonmagnetic impurity may be computed by ED in the sector of total spin $(S, S_z) = (1, 1)$ [this quantity vanishes identically in the singlet ground state $(0, 0)$], and is displayed for the 27-site cluster in Fig. 6. The site magnetizations exhibit a certain anticorrelation with the strength of the dimers formed on each bond, and thus have a tendency to oscillate with increasing distance from the impurity. The induced moments are particularly enhanced on sites far from the impurity, where different paths on the periodic cluster interfere, and the interference in this regime may even result in moments oriented opposite to the effective magnetic field (Figs. 6 and 7). The magnetization profile of the surrounding sites is the single most important consequence of impurities which is reflected in local-probe measurements of doped spin systems.

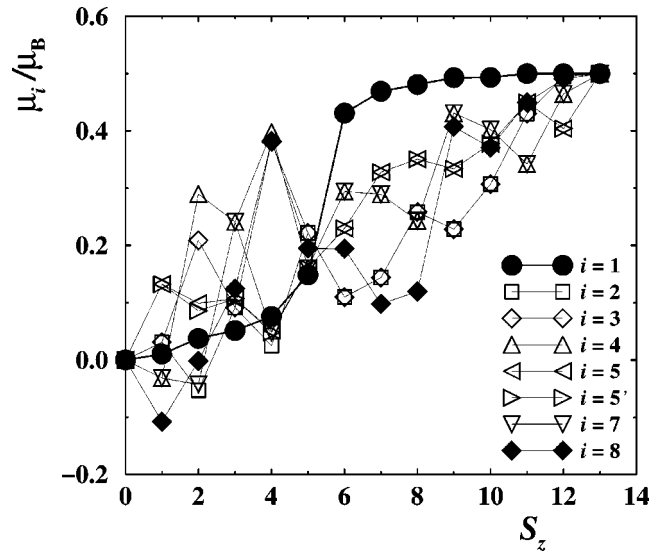


FIG. 7. Induced magnetization per site μ_i as a function of the spin sector S_z (analogous to an applied magnetic field) for all inequivalent sites (Ref. 23) neighboring an impurity, computed by ED for a 27-site cluster. With reference to the site labels in Fig. 6, the separate lines i represent first (4, 5, 23, 24), second (6, 9, 22, 25), third (10, 12, 19, 20), fourth (2, 3), equal fifth [(7, 8, 26, 27) and (13, 15, 16, 18)], seventh (14, 17), and eighth (11, 21) neighbors of the impurity site (1).

Figure 7 shows the magnetization per site induced by proximity to a nonmagnetic impurity for each spin sector obtainable by ED for a 27-site cluster. The spin sector may be considered as equivalent to an effective magnetic field which varies between zero ($S_z = 0$) and saturation ($S_z = 13$). The most pronounced variation is observed for the nearest-neighbor sites (filled circles in Fig. 7), which have very small magnetization at low fields because they are bound into the strong dimers frozen by the presence of the impurity on the same triangle. However, between $S_z = 4$ and $S_z = 6$ the moment shows an abrupt jump to saturation, implying the breaking and full polarization of these dimers at fields in excess of $1/3$ of the saturation field. We speculate that this behavior may be due to the presence of a particularly stable state of the remaining spins which corresponds to a $1/3$ magnetization plateau of the undoped kagome lattice.²⁴ The moments of the further-neighbor sites show a generally less systematic evolution, usually with a nonmonotonic character which implies a very significant rearrangement of the induced local magnetization as a function of field. This evolution is again marked by the most significant changes occurring close to the net magnetization value of $1/3$.

NMR has emerged as the technique of choice for analyzing in real space the effects of doped impurities on magnetizations and spin correlations. Information concerning these quantities is extracted from Knight-shifts, linewidth alterations, and, for certain cases, from relaxation times. A detailed NMR and nuclear quadrupole resonance analysis has been conducted recently for ^{71}Ga impurities in the kagome planes of the $S = 3/2$ spin system $\text{SrCr}_{9p}\text{Ga}_{12-9p}\text{O}_{19}$ (SCGO).¹⁵ While a quantitative determination of any shifts or linewidths depends on a detailed Hamiltonian for the hy-

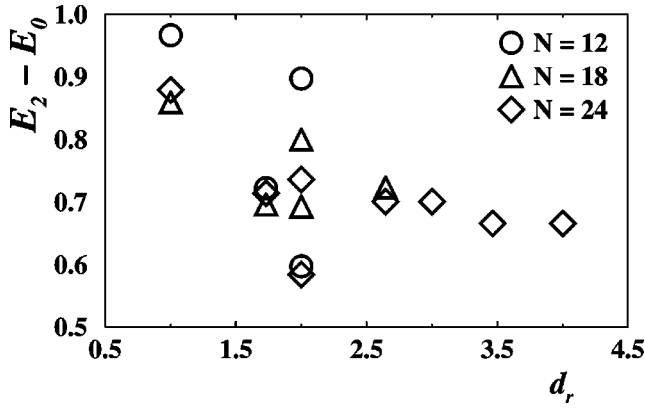


FIG. 8. Total energy E_2 for a pair of holes as a function of real hole separation d_r obtained by ED for clusters of 12, 18, and 24 sites with two impurities, shown relative to the impurity-free energy E_0 for the same clusters.

perfine interactions in a specific material, the results obtained in Fig. 7 may be considered as illustrative for the kagome geometry.

The important qualitative features are the absence of a single spin-1/2 degree of freedom anywhere in the vicinity of the impurity, and the rather large extent of the area of affected sites in spite of the very short spin-correlation lengths. The latter effect is contained in Fig. 7 in that the induced site magnetization values on the vertical axis are directly proportional to the peak shifts measured in a NMR field sweep. Impurities in the kagome lattice therefore produce a large number of satellite peaks.

Finally, with regard to the fact that most known kagome systems, including SCGO, are not $S=1/2$, there remain rather few studies of this geometry for higher values of the spin.^{24,25} On rather general grounds based on the geometry of the lattice, one expects that both triangles and depleted triangles retain the integral or half-integral nature of the spin per site. Thus it is at least plausible that the results for the $S=1/2$ system are directly relevant to higher half-integral-spin systems such as SCGO.²⁶

IV. HOLE REPULSION

In this section we present results characterizing the behavior of an even-site cluster doped with two impurities. A comparison with the undisturbed system⁴ reveals that the total energy not only increases in the presence of impurities, but increases further as the impurities are brought closer together. This effective hole repulsion is evident from the ED results of Fig. 8, which shows as a function of separation in real space the energies of all different two-hole states available for the relevant system sizes. Such a repulsive interaction between holes is most unusual in low-dimensional spin systems,^{17,28} and in fact we are unaware of analogous results for any model other than the frustrated chain.²⁹ The mutual repulsion of holes constitutes the central result of our analysis: particularly in the context of short-range RVB wave functions, it contradicts directly the most straightforward expectation for the behavior of doped holes, namely that when

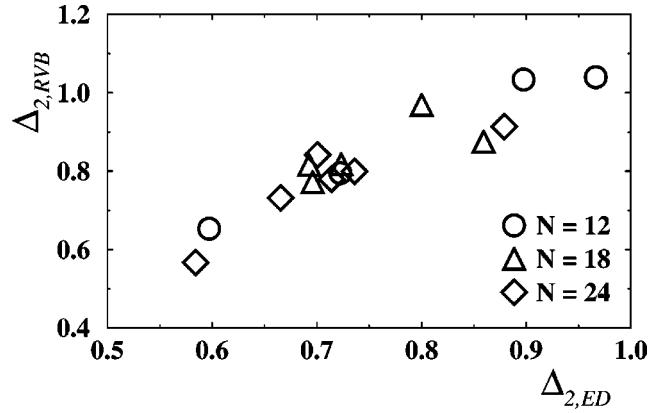


FIG. 9. Comparison of energies $\Delta_{2,ED}$ and $\Delta_{2,RVB}$ obtained, respectively, from ED and from calculations in the dimer-RVB basis for pairs of holes of different separations on clusters of 12, 18, and 24 sites with two impurities.

mobile these would choose to minimize the net disruption of the system by occupying the same dimer, and thus would exhibit a pairing attraction.³⁰ The consequences for mobile impurities with repulsive interactions may be expected to include hole crystallization, phase separation, and the possibility of transitions between metallic and insulating phases, and would bear considerable further investigation.

Although the total energy rises in the presence of impurities (Fig. 8), we comment that, as a consequence of the relatively large number of bonds removed, the energy per bond remaining in the doped system is in fact more strongly negative. Thus in the presence of impurities which break the lattice symmetry, the gains in dimerization energy for those bonds which are enhanced render the locally “frozen” dimer configurations of Sec. III more favorable than the resonating state of unconstrained dimers. One may speculate that the origin of this result lies in the action of the spinless impurity sites as “defects” which relieve the frustration by reducing the number of “defect triangles” (Ref. 31).

The increased total energy of two-hole states leads to a further observation in the context of the discussion (Sec. II) of the possibility that the ground state is a nondegenerate valence-bond crystal. The Hamiltonian [Eq. (1)] may be expressed as $H = H' + H''$, where

$$H' = J \sum_{\langle i\eta \rangle} \mathbf{S}_i^{\text{imp}} \cdot (\mathbf{S}_\eta^1 + \mathbf{S}_\eta^2) \quad (3)$$

denotes the four pairs of bonds from the impurity sites i to the two spins on the neighboring bonds η (we omit the generalization to include the case where the two impurities are themselves neighbors), and H'' denotes all bonds not involving an impurity site. Let $|\Psi_0\rangle$ be the ground state of the system in the absence of impurities and $|\Psi_2\rangle$ be the ground state with two impurities in a given configuration, then

$$H|\Psi_0\rangle = E_0|\Psi_0\rangle, \quad H''|\Psi_2\rangle = E_2|\Psi_2\rangle, \quad (4)$$

where E_0 and E_2 are the corresponding ground-state energies. Now, because the wave function $|\Psi_2\rangle$ represents a system with very strong, “frozen” dimerization on all of the

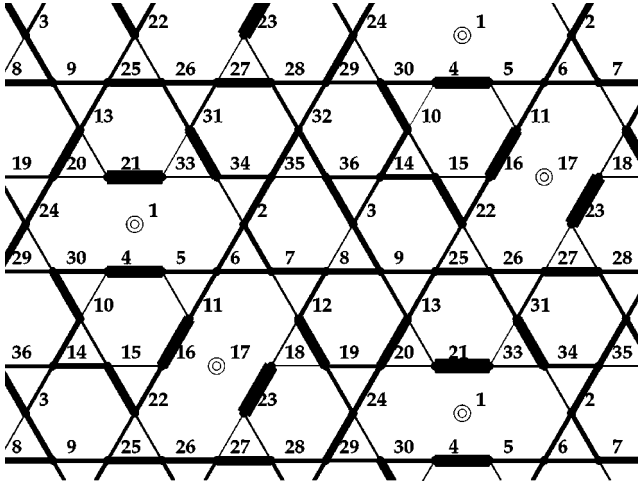


FIG. 10. Bond spin-spin correlations for two impurities in a 36-site cluster, obtained in the dimer-RVB basis. Bar width represents the strength of correlation functions for each bond on a linear scale where the largest value is -0.66 .

bonds η immediately surrounding the impurities (Sec. III and Fig. 4), the effect of H' [Eq. (3)] on this state is essentially zero, whence

$$H|\Psi_2\rangle \approx E_2|\Psi_2\rangle. \quad (5)$$

As a consequence of this relation, the fact (Fig. 8) that E_2 exceeds E_0 indicates that the ground state of the system with no impurities is indeed a resonating dimer liquid, and that a spontaneous freezing of particular patterns of dimer order²² may be excluded.

A. Dimer-RVB basis

We illustrate in Fig. 9 the efficacy of the dimer-RVB basis for the purpose of comparing ground-state energies. The correspondence between the dimer-RVB and ED results is shown by comparing the energies of all two-hole states in clusters of 12, 18, and 24 sites with two impurities, which represent all system sizes accessible by ED. Full details of the extraction of the energy values Δ_2 in Fig. 9 are given below. Although an inspection of the abscissas reveals that the agreement between individual pairs of values is not as convincing as for the spin-correlation functions (Sec. III), the main difference between the two sets of data may be reduced to a relative upward shift of all the RVB energies. The direct linear correlation between ED and dimer-RVB results (alluded to in Sec. II) demonstrates unambiguously that comparing the energies of different configurations of the two impurities, which is the primary goal of the energy analysis to follow, is a valid qualitative exercise when performed using the dimer-RVB results.

We show first the bond spin-spin correlation functions in the presence of a pair of impurities (Fig. 10). When considering the overlap of single-impurity dimerization patterns (Sec. III), it is evident that these are not fully mutually compatible. In fact, one finds by inspection that not only the configuration illustrated in Fig. 10 but all possible configurations of two impurities on the kagome lattice are in some

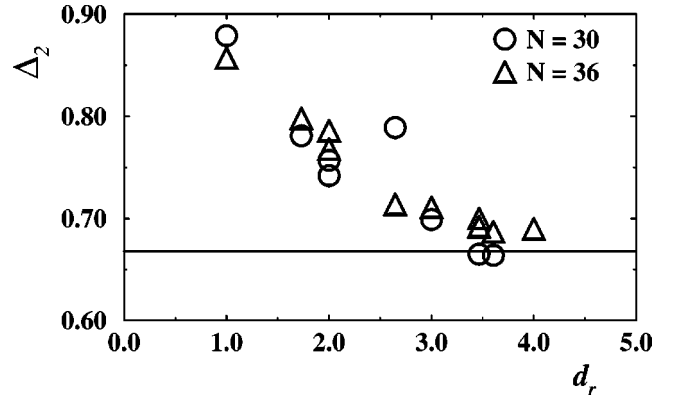


FIG. 11. Energies Δ_2 for two-hole states as a function of real hole separation for all configurations of two impurities on 30- and 36-site clusters, obtained by dimer-RVB calculations. The solid line marks twice the single-hole energy $2\Delta_1$ relevant for comparison, taken from the 33-site cluster.

measure incompatible. Comparison with other quantum spin systems suggests that this complete incompatibility is very specific to the kagome geometry, and its extent may be quantified by extracting the effective interaction energy of the holes (Fig. 11). In cluster calculations the frustration is also shown by the presence of relatively large local moments induced on the sites at the mismatch between dimerization regimes (cf. Fig. 6).

B. Interaction between impurities

Figure 11 shows twice the energy per hole as a function of separation for all configurations of two impurities on 30- and 36-site clusters, obtained in the dimer-RVB basis. We have analyzed the data in the following manner. As above, E_0 is the ground-state energy of each cluster in the absence of impurities, which is computed for even clusters and then extrapolated to odd clusters from the results for systems of sizes $N-3$ and $N+3$. E_1 is the ground-state energy in the presence of a single impurity, which is computed for odd clusters and extrapolated to even clusters from the results for systems of sizes $N-3$ and $N+3$. E_2 (above) is the ground-state energy with two impurities, and again may be computed directly for even clusters and extrapolated for odd clusters. We then define

$$\Delta_1 = E_1 - E_0 \quad (6)$$

as the energy of one hole,

$$\Delta_2 = E_2 - E_0 \quad (7)$$

as the energy of a two-hole state, and

$$\Delta_2 - 2\Delta_1 = E_2 - 2E_1 + E_0 \quad (8)$$

as the energy of interaction between two holes. Because of the extrapolation procedure it is important that the datasets for different system sizes be comparable. While certain problems arise for some system sizes due to the relatively large influence of the boundary conditions, we find the process to be valid for systems in excess of 27 sites. In this connection

we note that the two-hole energies Δ_2 shown in Fig. 11 are independent of the extrapolation between different system sizes, and it is only the direct comparison with Δ_1 for the 33-site system which requires validation of the procedure.

It is clear that the effective mutual repulsion decays only slowly. Because of the restricted sizes of the accessible clusters we are unable to speculate on the functional form of this decay, and in particular on the possibility that it may be long-ranged. We note only that for short distances (3–4 lattice constants) it appears to exhibit an approximate $1/d_r$ dependence, beyond which a steeper decrease is observed which may be either an intrinsic property of the interaction or a consequence of the system size. The form of the decay appears similar to that of the bond spin-correlation functions towards their undisturbed value [Fig. 5(b)].

At the phenomenological level, a repulsive interaction between two impurities may be understood from the preference for locally frozen dimer configurations. The dominant effect of increasing impurity separation lies in the reduction in strength of the partially frozen single-impurity dimerization patterns at the boundaries where they are forced to mesh, which reduces the corresponding energetic penalty; the interference of these patterns does not lead to their suppression and to a restoration of resonance energy. Given the slow decay of the dimer-dimer correlations, the possibility remains that the net repulsive interaction between holes could be long-ranged. Such an unexpected result may indeed be connected with a true deconfinement of spinonlike excitations for the kagome system, which would confirm speculation to this effect in 2D.^{18,21} We comment further on the issue of deconfinement below.

V. CONCLUSION

We have illustrated a variety of phenomena associated with the effects of static, spinless impurities doped into the $S=1/2$ antiferromagnetic Heisenberg model in kagome geometry. By analysis of spin-spin correlation functions and of the local magnetization patterns induced around impurities, we find that, despite the very short spin-spin correlation lengths of the highly frustrated system, dimer-dimer correlations develop over considerable distances due to a hole-induced freezing of their resonance. Furthermore, as a consequence of the continuum of states in the low-lying singlet manifold, there is no evidence for free local moments in the vicinity of impurity sites.

Most importantly, we have shown from the total energies of doped systems that impurities in the kagome lattice have an effective repulsive interaction, a phenomenon unique to our knowledge and in direct contradiction to the conven-

tional expectation for short-range RVB systems of a net pairing attraction. Furthermore, this effective repulsion is found to be rather long-ranged in nature, a most unusual result which is presumably related with the very strong frustration inherent to the kagome geometry.

Our comparisons of doping effects provide additional justification for the validity of the short-range dimer-RVB framework as a suitable description of the ground-state singlet manifold in the kagome antiferromagnet. We have shown that the dimer-RVB basis provides a valuable means of probing the nature of spin and charge degrees of freedom in a further class of quantum magnets. This realization of a highly resonant RVB state, arising as a consequence of the extremely frustrated nature of the system, also presents an important contrast to other low-dimensional spin systems which are known to be described by RVB-type wave functions, particularly with regard to the localization of free spins and to the pairing of holes.

We summarize only briefly the consequences of our analysis for experiment. The majority of known kagome materials do not have complete filling of the lattice sites by a single value of the spin S , and as such the study of impurities is a significant component of their characterization. Nonmagnetic impurities in the kagome lattice have the important property that they do not generate localized spins at the vacant site, and do generate by the nature of their extended range of influence a significant number of satellites for each peak. On heuristic grounds we believe that our analysis of the qualitative features to be expected in the $S=1/2$ system is relevant also for $S=3/2$, and perhaps for higher half-integral spins.

Finally, on the issue of deconfinement in highly frustrated systems of dimensionality higher than one, we have shown clearly from the presence of the mutual repulsive interaction between holes that charge degrees of freedom are deconfined. Further, the absence of localized $S=1/2$ degrees of freedom around vacancies in the lattice demonstrates that spin and charge are deconfined. However, on the question of whether the spin excitations of the undoped system are appropriately described by deconfined spinon excitations, our results do not provide a proof of this hypothesis.

ACKNOWLEDGMENTS

We are grateful to P. Sindzingre for helpful provision of ED spectra for undoped clusters, and to C. Lhuillier and G. Misguich for valuable discussions. This work was supported by the Swiss National Science Foundation and by the French Centre National de la Recherche Scientifique.

¹J.T. Chalker and J.F. Eastmond, Phys. Rev. B **46**, 14 201 (1992).

²P.W. Leung and V. Elser, Phys. Rev. B **47**, 5459 (1993).

³C. Zeng and V. Elser, Phys. Rev. B **51**, 8318 (1995).

⁴P. Lecheminant, B. Bernu, C. Lhuillier, L. Pierre, and P. Sindzingre, Phys. Rev. B **56**, 2521 (1997); C. Waldtmann, H.-U.

Everts, B. Bernu, C. Lhuillier, P. Sindzingre, P. Lecheminant, and L. Pierre, Eur. Phys. J. B **2**, 501 (1998).

⁵F. Mila, Phys. Rev. Lett. **81**, 2356 (1998).

⁶M. Mambrini and F. Mila, Eur. Phys. J. B **17**, 651 (2000).

⁷D.S. Rokhsar and S.A. Kivelson, Phys. Rev. Lett. **61**, 2376

- (1988).
- ⁸R. Moessner and S.L. Sondhi, Phys. Rev. Lett. **86**, 1881 (2001).
- ⁹G. Misguich, D. Serban, and V. Pasquier, Phys. Rev. Lett. **89**, 137202 (2002); Phys. Rev. B **67**, 214413 (2003).
- ¹⁰G. Misguich, B. Bernu, C. Lhuillier, and C. Waldtmann, Phys. Rev. Lett. **81**, 1098 (1998); W. LiMing, G. Misguich, P. Sindzingre, and C. Lhuillier, Phys. Rev. B **62**, 6372 (2000).
- ¹¹A.S. Wills, A. Harrison, C. Ritter, and R.I. Smith, Phys. Rev. B **61**, 6156 (2000).
- ¹²A. Keren, K. Kojima, L.P. Le, G.M. Luke, W.D. Wu, Y.J. Uemura, M. Takano, H. Dabkowska, and M.J.P. Gingras, Phys. Rev. B **53**, 6451 (1996).
- ¹³S.-H. Lee, C. Broholm, M.F. Collins, L. Heller, A.P. Ramirez, Ch. Kloc, E. Bucher, R.W. Erwin, and N. Laceyvic, Phys. Rev. B **56**, 8091 (1997).
- ¹⁴Z. Hiroi, M. Hanawa, N. Kobayashi, M. Nohara, H. Takagi, Y. Kato, and M. Takigawa, J. Phys. Soc. Jpn. **70**, 3377 (2001).
- ¹⁵L. Limot, P. Mendels, G. Collin, C. Mondelli, B. Ouladdiaf, H. Mutka, N. Blanchard, and M. Mekata, Phys. Rev. B **65**, 144447 (2002), and references therein.
- ¹⁶M. Laukamp, G.B. Martins, C. Gazza, A.L. Malvezzi, E. Dagotto, P.M. Hansen, A.C. Lopez, and J. Riera, Phys. Rev. B **57**, 10 755 (1998).
- ¹⁷N. Bulut, D. Hone, D.J. Scalapino, and E.Y. Loh, Phys. Rev. Lett. **62**, 2192 (1989).
- ¹⁸S. Sachdev and M. Vojta, in *Proceedings of the XIII International Congress on Mathematical Physics*, edited by A. Fokas, A. Grigoryan, T. Kibble, and B. Zegarliniski (International Press, Boston, 2001).
- ¹⁹B. Normand and F. Mila, Phys. Rev. B **65**, 104411 (2002).
- ²⁰S. Sachdev, Phys. Rev. B **45**, 12 377 (1992).
- ²¹P. Sindzingre, C. Lhuillier, and J.-B. Fouet, *Advances in Quantum Many-Body Theory* (World Scientific, Singapore, 2002), Vol. 5, p. 90.
- ²²A.V. Syromyatnikov and S.V. Maleyev, cond-mat/0304570 (unpublished); P. Nikolic and T. Senthil, cond-mat/0305189 (unpublished).
- ²³The behavior of the number of inequivalent sites as a function of the spin sector arises from the presence of an additional permutation symmetry among the sites for the 27-site cluster with the chosen boundary conditions. This symmetry does not in general commute with the two reflection symmetries of the cluster, and so cannot be obtained simultaneously with these. However, in the majority of spin sectors it is possible to obtain all three symmetries simultaneously, making sites $i=2$ and 3 , $i=5$ and $5'$, and $i=4$ and 7 equivalent in these cases.
- ²⁴K. Hida, J. Phys. Soc. Jpn. **70**, 3673 (2001); D.C. Cabra, M.D. Grynberg, P.C.W. Holdsworth, and P. Pujol, Phys. Rev. B **65**, 094418 (2002); J. Schulenburg, A. Honecker, J. Schnack, J. Richter, and H.-J. Schmidt, Phys. Rev. Lett. **88**, 167207 (2002).
- ²⁵K. Hida, J. Phys. Soc. Jpn. **69**, 4003 (2000); I. Rudra, D. Sen, and S. Ramasesha, cond-mat/0210122 (unpublished).
- ²⁶A further heuristic justification for the relevance of the current results at least to the $S=3/2$ case may be obtained by considering that the kagome geometry supports a nondegenerate valence-bond-solid state (Ref. 27) for spins $S=2$. In a RVB basis a system of spins $S=3/2$ is equivalent to a set of dimer vacancies in this background which have exactly the same degeneracy as the dimers in the $S=1/2$ system.
- ²⁷I. Affleck, T. Kennedy, E. Lieb, and H. Tasaki, Phys. Rev. Lett. **59**, 799 (1987); Commun. Math. Phys. **115**, 477 (1988).
- ²⁸E. Dagotto, J. Riera, and D. Scalapino, Phys. Rev. B **45**, 5744 (1992).
- ²⁹Reexamination of results obtained by two of the authors (Ref. 19) reveals that a mutual repulsion of impurities also occurs in the spin chain with frustrating next-neighbor interactions.
- ³⁰P.W. Anderson, Science **235**, 1196 (1987).
- ³¹V. Elser, Phys. Rev. Lett. **62**, 2405 (1989).